Longitudinal Vibration of CNTs Viscously Damped in Span

Mustafa Arda [a] and Metin Aydogdu [b]*

[a,b]Trakya University, Department of Mechanical Engineering
[*]E-mail address: mustafaarda@trakya.edu.tr

Abstract

In this study, longitudinal vibration of a carbon nanotube with an attached damper has been investigated using the nonlocal stress gradient elasticity theory. Equations of motions have been solved analytically and frequencies of clamped-clamped and clamped-free nanotubes have been obtained explicitly in terms of damping coefficient, nonlocal parameter, the attachment point of damper and nanotube length. The nonlocal effects have important effects on the dynamics of a CNT with an attached damper.

Keywords: longitudinal vibration; viscously damped; carbon nanotubes; nonlocal elasticity

1. Introduction

Discovery of carbon nanotubes (CNTs) by Iijima [1] has important results on nanotechnology. With superior properties like electrical and heat conductivity, strength, density etc., scientists have considered use of CNTs in many areas: nano-electromechanical devices, nano-pharmaceutical products, nano-bearings, nano-sensors, etc.

Dynamic behavior of CNTs at different areas is very important in design of nano-products. Nowadays, scientists try to use CNTs in medical applications [2,3], bearing-like products [4,5], electromagnetic damping process [6] and molecular transportation [7,8] etc.

Generally, two modeling techniques are used in nano-mechanics: continuum model and discrete model. Because of the size independence, classical theories are not suitable at nanoscale. Nonlocal Elasticity, a modified continuum model, was firstly proposed by Eringen [9,10]. In this theory mechanical behavior of materials is size dependent. Also Molecular Dynamics (MD) Simulations are used as a discrete model in nano-mechanics. Both models give more acceptable results than the classical theory when compared to the lattice dynamics results.

Recently, wave propagation in SWCNTs has been compared for the nonlocal continuum models and MD Simulations [11]. Very close results were obtained between two results. Lattice Dynamic results for longitudinal wave propagation in nanotubes have been investigated in previous studies [12].

Thermal, concentration or electromagnetic fields can cause a damping effect on CNTs [13] . Wang et al. [14] have studied asymmetric vibration of a single-walled carbon nanotubes (SWCNTs) immersed in water. Assuming that, water can establish a viscous damping effect on axisymmetric radial,

longitudinal and torsional vibration. Rinaldi et al. [15] investigated the fluid conveying micro scale pipes with the effects of flow velocity on damping, stability and frequency shift. Vibration and instability analysis of CNTs with a fluid flow is studied by Ghavanloo et al. [16] and microtubules in surrounding cytoplasm is investigated by Ghavanloo et al. [17]. In plane and flexural vibration of fluid conveying CNTs in viscoelastic medium is studied by [18] and in viscous fluid is studied by Ghavanloo et al. [19]. Yun et al. [20] have obtained the free vibration and flow-induced flutter instability of fluid conveying multi-walled carbon nanotubes (MWCNTs). Vibrations and instability of fluid conveying double-walled carbon nanotubes (DWCNTs) is studied using the modified couple stress theory by Zeighampour and Tadi Beni [21]. Martin and Houston [22] investigated the gas damping effect on CNT based nano-resonator operating in low vacuum conditions. The natural frequencies of aligned SWCNT reinforced composite beams were obtained using shear deformable composite beam theories by Aydogdu [23]. Chemi et al. [24] investigated elastic buckling of chiral DWCNTs under axial compression. Longitudinal forced vibration of nanorods studied by Aydogdu and Arda [25] using the nonlocal elasticity theory of Eringen. They considered uniform, linear and sinusoidal loads on axial direction.

One of the possible medical applications of CNTs is the viscous fluid conveying SWCNT embedded in biological soft tissue. Transverse vibrational model is studied by Soltani et al. [26]. They simulated the viscoelastic behavior of surrounding tissue using Kevin-Voigt model. In addition to mentioned work, transverse vibration of fluid conveying DWCNTs embedded in biological soft tissue is investigated by Zhen et al. [27].

Hoseinzadeh and Khadem [28] studied the thermoelastic vibration and damping of DWCNT upon interlayer van der Waals interaction and initial axial stress. Same authors also investigated the thermoelastic vibration behavior and damping of DWCNTs using nonlocal shell theory [29]. Thermoelastic damping in a DWCNT under electrostatic actuation is obtained through an analytical method by Hajnayeb and Khadem [30].

Magnetic damping effect on CNTs as a nanoelectromechanical resonators is studied by Schmid et al. [31] at cryogenic temperature. Chang and Lee [32] investigated vibration behavior of CNTs using non-local viscoelasticity theory including thermal and foundation effects.

Damping effect on rods for various boundary conditions is investigated at macro scale by [33–35]. Viscoelastic properties of SWCNTs are investigated with a semi-analytical approach and associated damping mechanism at nano scale by Zhou et al. [36]. Jeong et al. [37] modeled the nonlinear damping behavior of micro cantilever-nanotube system and compared with measurement results. Adhikari et al. [38] investigated free and forced axial vibrations of strain-rate depended viscous damping and velocity dependent viscous damped nonlocal rods. The asymptotic frequencies of four kinds of nonlocal viscoelastic damped structures, including an Euler-Bernoulli beam with rotary inertia, a Timoshenko beam, a Kirchhoff plate with rotary inertia and a Mindlin plate are studied by Lei et al. [39]. Arani et al. [40] investigated the vibration of double viscoelastic CNTs conveying viscous fluid coupled by visco-Pasternak medium using the surface nonlocal theory. Karličić et al. [41] studied free longitudinal vibration of a nonlocal viscoelastic double-nanorod system as a complementary study at nano scale to Erol and Gürgöze's paper [42].

Mechanical response of a CNT atomic force microscope (AFM) probe tip contact is an important problem (Fig.1). This response can be modeled as a spring [43] or damping element according continuum mechanics. Damping of a mechanical resonators based on CNTs is studied by Eichler et al. [44]. Li et al. [45] investigated the mechanical oscillatory behaviors of MWCNT oscillators in gaseous environment using MD simulation. Suspended carbon nanotube resonators behavior over a broad range of temperatures to explore the physics of semi flexible polymers in underdamped

environments simulated by Barnard et al. [46]. Hüttel et al. [47] observed the transversal vibration mode of suspended CNTs at miliKelvin temperatures by measuring the single electron tunneling current. The measured magnitude and temperature dependence of the Q factor shown a remarkable agreement with the intrinsic damping predicted for a suspended carbon nanotube. According to author's literature knowledge, vibration of a nanorod with an attached viscous damper has not been considered in the previous studies.
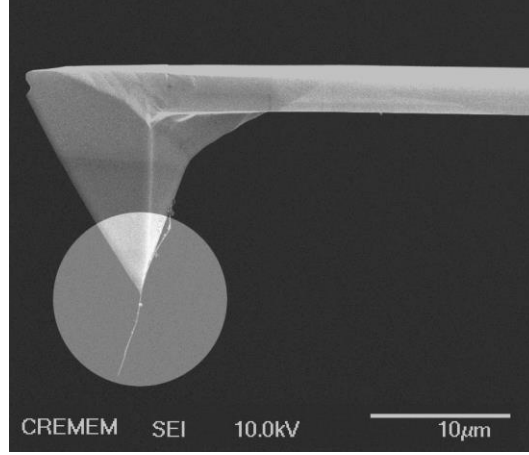
Fig. 1. SEM Image of a MWCNT Attached to Pyramidal Si Tip [43]

2. Analysis

A nanorod of length L and diameter ϕ is considered. A viscous damper is attached at an arbitrary point of the rod (Fig. 2). The equation of motion in the longitudinal direction can be expressed as:

$$EA\frac{\partial^2 u}{\partial x^2} = m\frac{\partial^2 u}{\partial t^2} \tag{1}$$

where *A* is the cross-section area , *E* is the Young Modulus and m is the mass per unit length. In Fig. (2), η defines the attachment point of the viscous damper, *L* is the length of nanorod, *d* is the damping coefficient of viscous damper and *u(x,t)* is the displacement in longitudinal direction.

2.1. Equation of motion of nanorod in nonlocal model

The nonlocal constitute relation can be given as [9,10] :

$$(1 - \mu\nabla^2)\tau_{kl} = \lambda\varepsilon_{rr}\delta_{kl} + 2G\varepsilon_{kl} \tag{2}$$

where τ_{kl} is the nonlocal stress tensor, ε_{kl} is the strain tensor, λ and *G* are the lame constants, $\mu=(e_0 a)^2$. μ *is* called the nonlocal parameter, *a* is an internal characteristic length and e_0 is a constant. In this study, $\mu \leq 2nm^2$ is accepted for SWCNTs. Using the Nonlocal Elasticity Theory in one dimensional form leads following equation of motion:

$$EA\frac{\partial^2 u}{\partial x^2} = \left(1 - \mu\frac{\partial^2}{\partial x^2}\right)m\frac{\partial^2 u}{\partial t^2} \tag{3}$$

If the nonlocal parameter μ is assumed identically zero, Eq. (3) reduces to classical rod model. In order to study the equation of motion of a nanorod with an attached viscous damper, the nanorod is divided into two parts. The equation of motion for each segment can be written as:

$$EA\frac{\partial^2 u_i}{\partial x^2} = \left(1 - \mu\frac{\partial^2}{\partial x^2}\right)m\frac{\partial^2 u_i}{\partial t^2} \quad , \quad (i = 1,2) \tag{4}$$

where u_1 and u_2 denote displacement of the left and the right segments of the nanorod respectively. The corresponding boundary and continuity conditions are written as:
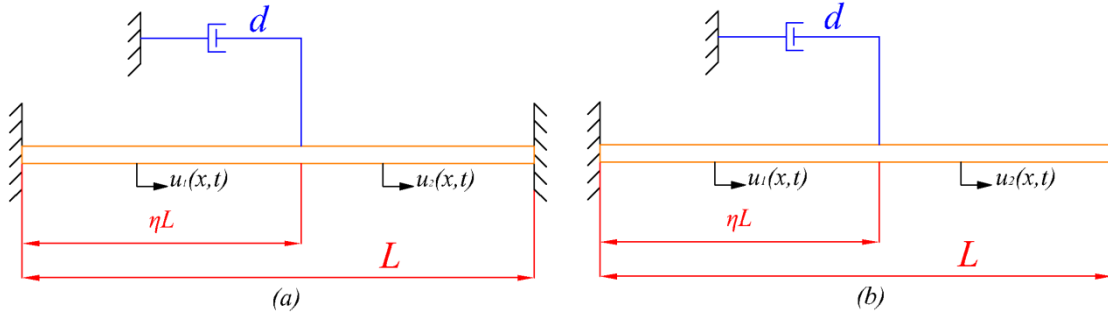
Fig. 2 Nanorod model with a viscous damper in a)C-C boundary condition b)C-F boundary condition

Clamped-Clamped (C-C):

$$u_1(0,t) = 0,$$
$$u_1(\eta L,t) = u_2(\eta L,t),$$
$$EA\frac{\partial u_1(\eta L,t)}{\partial x} + \mu m\frac{\partial^3 u_1(\eta L,t)}{\partial x\,\partial t^2} - EA\frac{\partial u_2(\eta L,t)}{\partial x} - \mu m\frac{\partial^3 u_2(\eta L,t)}{\partial x\,\partial t^2} + d\frac{\partial u_1(\eta L,t)}{\partial t} - \mu d\frac{\partial^3 u_1(\eta L,t)}{\partial x^2\,\partial t} = 0,$$
$$u_2(L,t) = 0 \tag{5}$$

Clamped-Free (C-F):

$$u_1(0,t) = 0,$$

$$u_1(\eta L,t) = u_2(\eta L,t),$$

$$EA\frac{\partial u_1(\eta L,t)}{\partial x} + \mu m\frac{\partial^3 u_1(\eta L,t)}{\partial x\,\partial t^2} - EA\frac{\partial u_2(\eta L,t)}{\partial x} - \mu m\frac{\partial^3 u_2(\eta L,t)}{\partial x\,\partial t^2} + d\frac{\partial u_1(\eta L,t)}{\partial t} - \mu d\frac{\partial^3 u_1(\eta L,t)}{\partial x^2\,\partial t} = 0,$$

$$EA\frac{\partial u_2(L,t)}{\partial x} + \mu m\frac{\partial^3 u_2(L,t)}{\partial x\,\partial t^2} = 0 \tag{6}$$

The longitudinal displacement u_i can be expressed as:

$$u_i(x,t) = U_i(x)\,e^{\lambda t} \quad , \quad (i = 1,2) \tag{7}$$

where $U_i(x)$ and λ is the amplitude function and characteristic value respectively. Inserting Eq.(7) into Eq.(4) gives following dimensionless equations of motion:

$$\frac{\partial^2 U_i}{\partial x^2} - \beta^2 U_i = 0 \quad , \quad (i = 1,2) \tag{8}$$

where:

$$\beta^2 = \frac{m\lambda^2}{EA + \mu m\lambda^2} \tag{9}$$

25

The solutions of Eq.(8) are:

$$U_1(x) = C_1 e^{\beta x} + C_2 e^{-\beta x} \tag{10}$$
$$U_2(x) = C_3 e^{\beta x} + C_4 e^{-\beta x} \tag{11}$$

where C_1, C_2, C_3 and C_4 are the undetermined coefficients. For the C-C boundary condition, eigenvalue equation is obtained using Eq.(5), Eq.(10) and Eq.(11):

$$\begin{bmatrix} CC_{11} & CC_{12} & CC_{13} & CC_{14} \\ CC_{21} & CC_{22} & CC_{23} & CC_{24} \\ CC_{31} & CC_{32} & CC_{33} & CC_{34} \\ CC_{41} & CC_{42} & CC_{43} & CC_{44} \end{bmatrix} \begin{bmatrix} C_1 \\ C_2 \\ C_3 \\ C_4 \end{bmatrix} = 0 \tag{12}$$

where

$$CC_{11} = 1 \ , \quad CC_{12} = 1 \ , \quad CC_{13} = 0 \ , \quad CC_{14} = 0 \ ,$$
$$CC_{21} = 0 \ , \quad CC_{22} = 0 \ , \quad CC_{23} = e^{\beta L} \ , \quad CC_{24} = e^{-\beta L} \ ,$$
$$CC_{31} = e^{\beta \eta L} \ , \quad CC_{32} = e^{-\beta \eta L} \ , \quad CC_{33} = -e^{\beta \eta L} \ , \quad CC_{34} = -e^{\beta \eta L}$$
$$CC_{41} = e^{\beta \eta L} \left(1 + \alpha + D(1 - \mu\beta^2)^{1/2} \right) \ ,$$
$$CC_{42} = e^{-\beta \eta L} \left(-1 - \alpha + D(1 - \mu\beta^2)^{1/2} \right) \ ,$$
$$CC_{43} = e^{\beta \eta L}(-1 - \alpha) \ ,$$
$$CC_{44} = e^{-\beta \eta L}(1 + \alpha) \tag{13}$$

and for the C-F boundary condition, eigenvalue equation is obtained using Eq.(6), Eq.(10) and Eq.(11):

$$\begin{bmatrix} CF_{11} & CF_{12} & CF_{13} & CF_{14} \\ CF_{21} & CF_{22} & CF_{23} & CF_{24} \\ CF_{31} & CF_{32} & CF_{33} & CF_{34} \\ CF_{41} & CF_{42} & CF_{43} & CF_{44} \end{bmatrix} \begin{bmatrix} C_1 \\ C_2 \\ C_3 \\ C_4 \end{bmatrix} = 0 \tag{14}$$

where

$$CF_{11} = 1 \ , \quad CF_{12} = 1 \ , \quad CF_{13} = 0 \ , \quad CF_{14} = 0 \ ,$$
$$CF_{21} = 0 \ , \quad CF_{22} = 0 \ , \quad CF_{23} = (1 + a)e^{\beta L} \ , \quad CF_{24} = (-1 - a)e^{-\beta L} \ ,$$
$$CF_{31} = e^{\beta \eta L} \ , \quad CF_{32} = e^{-\beta \eta L} \ , \quad CF_{33} = -e^{\beta \eta L} \ , \quad CF_{34} = -e^{\beta \eta L} \ ,$$
$$CF_{41} = e^{\beta \eta L} \left(1 + \alpha + D(1 - \mu\beta^2)^{1/2} \right) \ ,$$
$$CF_{42} = e^{-\beta \eta L} \left(-1 - \alpha + D(1 - \mu\beta^2)^{1/2} \right) \ ,$$
$$CF_{43} = e^{\beta \eta L}(-1 - \alpha) \ ,$$
$$CF_{44} = e^{-\beta \eta L}(1 + \alpha) \tag{15}$$

For a nontrivial solution the determinant of the coefficient matrix in Eq.(12) and Eq.(14) must be zero. If these determinant equations are rearranged, following characteristic equations are obtained for each boundary conditions considered:

$$2(\alpha + 1)\sinh(\bar{\beta}) + D\left(1 - \frac{\mu}{L^2}\bar{\beta}^2\right)^{\frac{1}{2}} \left\{ \cosh(\bar{\beta}) - \cosh[(1 - 2\eta)\bar{\beta}] \right\} = 0 \ \rightarrow \ (C - C) \tag{16}$$

$$2(\alpha + 1)\cosh(\bar{\beta}) + D\left(1 - \frac{\mu}{L^2}\bar{\beta}^2\right)^{\frac{1}{2}} \left\{ \sinh(\bar{\beta}) - \sinh[(1 - 2\eta)\bar{\beta}] \right\} = 0 \ \rightarrow \ (C - F) \tag{17}$$

where

$$\alpha = \frac{\mu}{L^2} \frac{\bar{\beta}^2}{\left(1 - \frac{\mu}{L^2}\bar{\beta}^2\right)} \quad , \quad D = \frac{dc}{EA} \quad , \quad c = \sqrt{\frac{E}{\rho}} \quad , \quad \bar{\beta} = \beta L \qquad (18)$$

where α is the dimensionless coefficient, D is the dimensionless damping coefficient, c is the velocity of the wave propagation along the nanorod and $\bar{\beta}$ is the dimensionless characteristic parameter. $\bar{\beta}$ is a complex number and its imaginary part defines the non-dimensional frequency (NDF) and real part defines the non-dimensional damping coefficient (NDD) of nanorod. Damping ratio (ξ) of nanorod is defined in the following form:

$$\xi = \frac{|\text{NDD}|}{\sqrt{\text{NDF}^2 + \text{NDD}^2}} \qquad (19)$$

3. Numerical Results and Discussion

In this section, the non-dimensional frequency (NDF) and non-dimensional damping coefficient (NDD) of the nanorod are investigated for different dimensionless damping coefficient, nanotube length, nonlocal parameter and the attachment point of viscous damper. Geometrical and material properties of the CNT are taken from Ref. [48]. The validity of present work is checked in the next section.

3.1. Validation of the Present Results

By assuming nonlocal parameter is identically zero (μ=0), the local model solutions are obtained. The dimensionless characteristic values are compared with local model from Ref. [33] and Ref. [34] for C-C and C-F boundary conditions in Table 1. Good agreement is observed between two results.

Table 1 Comparison of characteristic values with literature ($\eta = 0.6$)

	Present Work		[34]	[33]
	C-C	C-F	C-C	C-F
$\bar{\beta}_1$	-0.020352+3.141619i	-0.001439+1.570796i	-0.020349+3.141619i	-0.001472+1.570796i
$\bar{\beta}_2$	-0.007773+6.283168i	-0.000210+4.712389i	-0.007772+6.283168i	-0.000214+4.712389i
$\bar{\beta}_3$	-0.007773+9.424794i	-0.002200+7.853981i	-0.007772+9.424794i	-0.002249+7.853981i

3.2. Dimensionless Damping Effect on NDF and NDD

In Figs. (3-14) and Tables (2-3), variations of NDF and NDD with dimensionless damping coefficient for C-C and C-F boundary condition are depicted. According to these results following conclusions are obtained:

The fundamental NDF value increases but the second and third NDF decrease with increasing D for the C-C boundary condition. However, for the C-F boundary condition, variation of NDF depends on η. First and second NDF increase whereas third NDF decreases with increasing D when $\eta < 0.5$. On the other hand, first and second NDF decrease and third NDF increase with increasing D when $\eta > 0.5$ (See Table (2) and (3)). Generally, NDD increases with increasing D except for some cases. For smaller nanotube length, nonlocal effect is more pronounced and it reduces the NDD (See Figs. (4) and (6)).

NDF decreases with increasing the nonlocal parameter for both C-C and C-F boundary condition. The nonlocal effect decreases with increasing nanotube length. NDD increases with increasing μ for both C-C and C-F boundary condition (See Figs. (3-10)).

The attachment point of damper has different effects on NDF for C-C and C-F cases. In C-C boundary condition, fundamental NDF decreases, however second and third NDF increase when $\eta < 0.5$. The obtained results for NDF and NDD are symmetric with respect to $\eta = 0.5$ (i.e. results of $\eta = 0.1$ are equal to $\eta = 0.9$, etc.). The NDD is maximum at $\eta = 0.5$.
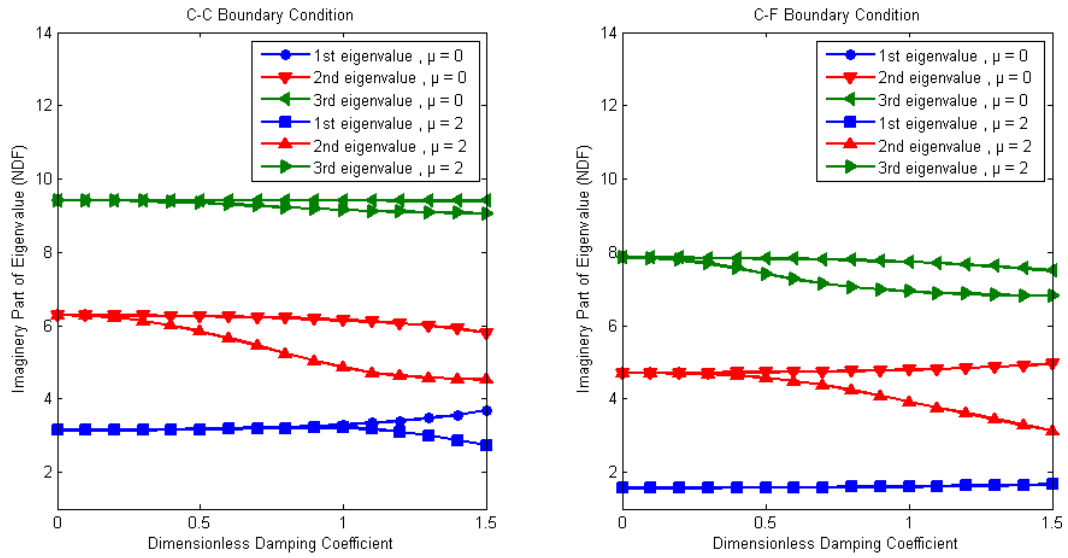
Fig. 3. Variation of NDF with dimensionless damping coefficient ξ ($\eta = 0.3$, L = 10 nm)
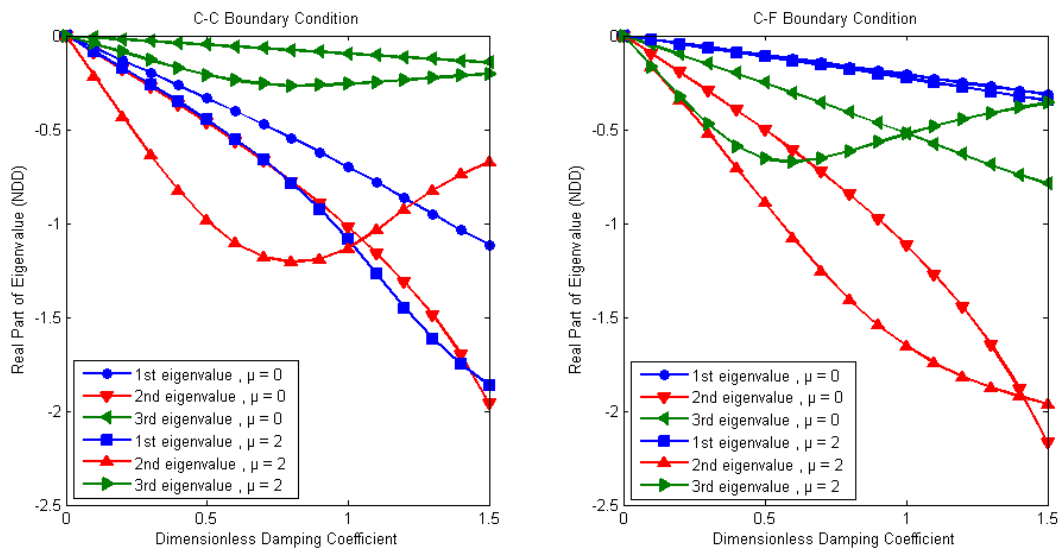
Fig. 4. Variation of NDD with dimensionless damping coefficient ξ ($\eta = 0.3$, L = 10 nm)
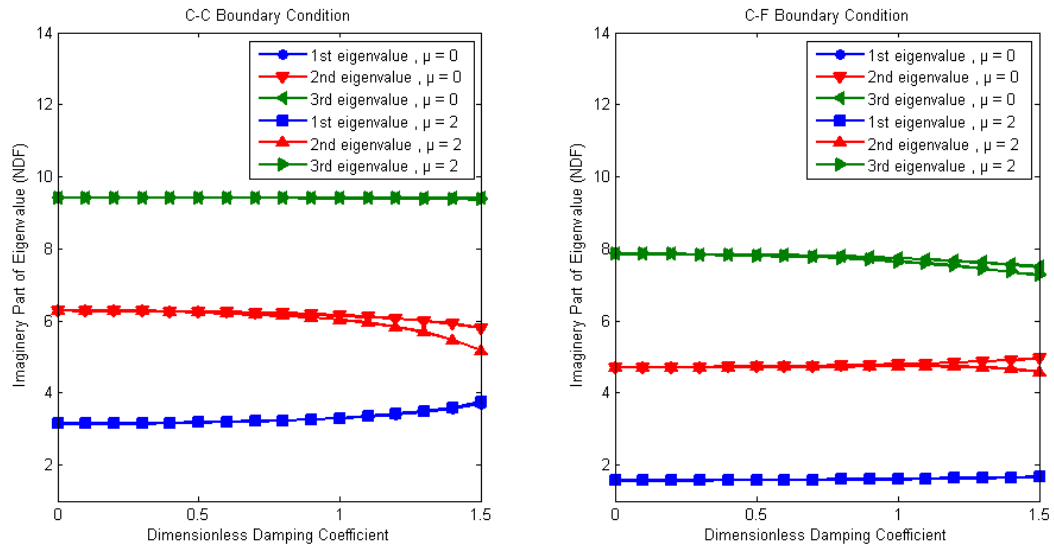
Fig. 5. Variation of NDF with dimensionless damping coefficient ξ (η = 0.3 , L = 30 nm)
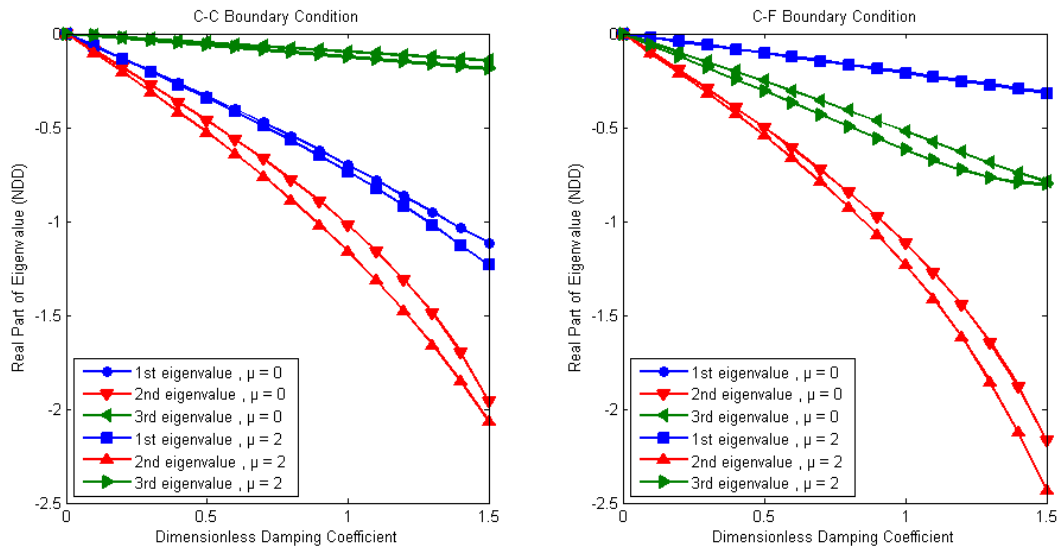
Fig. 6. Variation of NDD with dimensionless damping coefficient ξ (η = 0.3 , L = 30 nm)
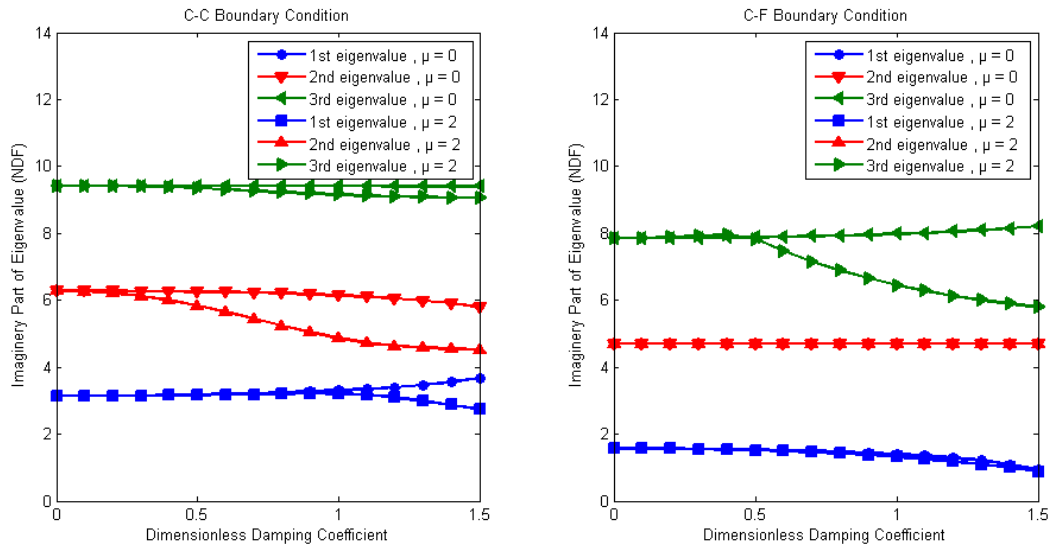
Fig. 7. Variation of NDF with dimensionless damping coefficient ξ ($\eta = 0.7$, L = 10 nm)
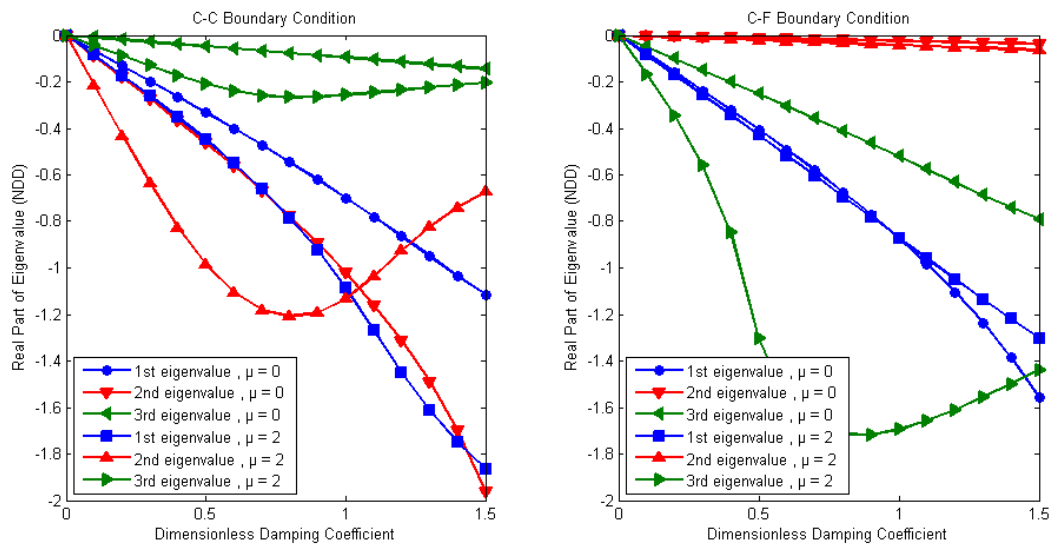
Fig. 8. Variation of NDD with dimensionless damping coefficient ξ ($\eta = 0.7$, L = 10 nm)
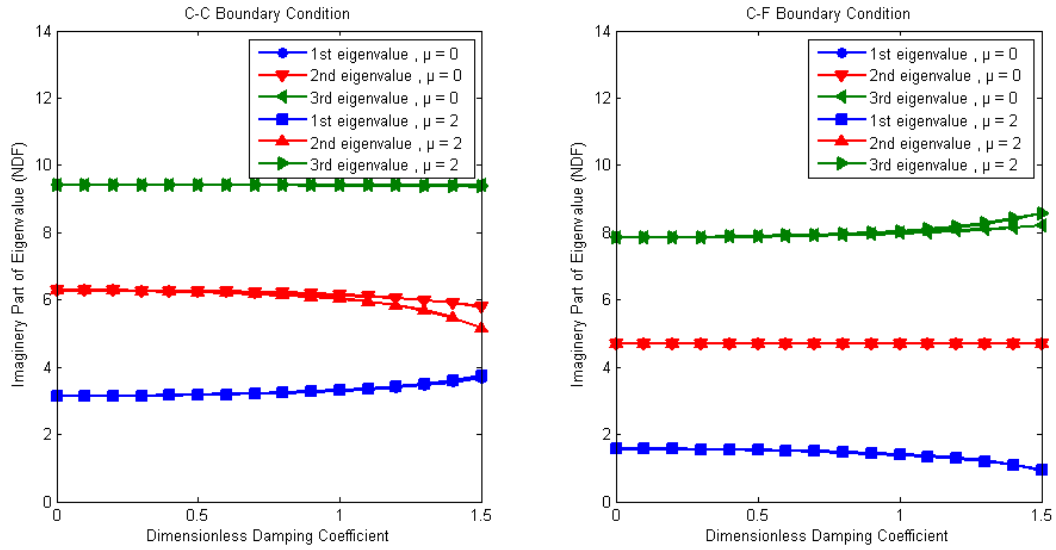
Fig. 9. Variation of NDF with dimensionless damping coefficient ξ ($\eta = 0.7$, L = 30 nm)
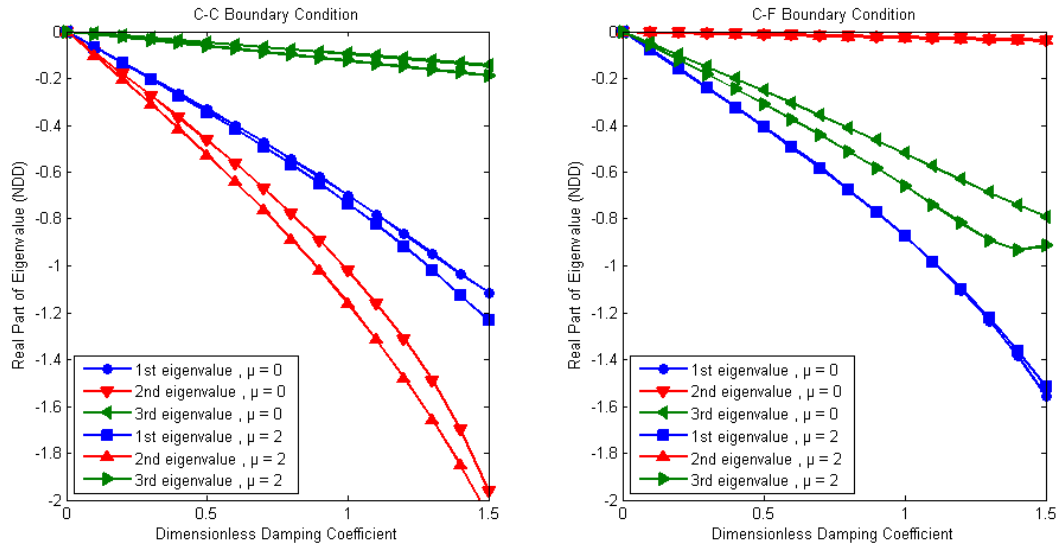
Fig. 10. Variation of NDD with dimensionless damping coefficient ξ ($\eta = 0.7$, L = 30 nm)

For the C-F boundary condition, first and second NDF decreases and third NDF increases with increasing η and reaches a maximum value at $\eta = 1$ (See Table (2) and (3)).

Nanotube length has effect on NDF and NDD only for the nonlocal results. The local results ($\mu=0$) are not affected by change of nanotube length (See Table (2) and (3)). This is an expected result from the classical theory. The NDF increases and the NDD decreases with increasing nanotube length in the nonlocal case.

Damping ratio (ξ) increases with increasing dimensionless damping coefficient (D) generally. Attachment point of damper increases damping ratio in C-F case when η is approaching to 1. In C-C case, damping ratio reaches maximum value at $\eta = 0.5$. For longer nanotube length, local and nonlocal damping ratios have very close values, since bigger nanotube length reduces the nonlocal effect.

Table 2 Characteristic values of nanorod for C-C boundary condition

η	L (nm)		Dimensionless Damping Coefficient (D)			
			ξ = 0.5		ξ = 1.5	
			μ=0 nm²	μ=2 nm²	μ=0 nm²	μ=2 nm²
0.3	10	$\overline{\beta_1}$	-0.3326+3.1744i	-0.4490+3.1663i	-1.1147+3.6824i	-1.8652+2.7424i
		$\overline{\beta_2}$	-0.4647+6.2550i	-0.9872+5.8387i	-1.9599+5.7909i	-0.6720+4.5281i
		$\overline{\beta_3}$	-0.0478+9.4219i	-0.2102+9.3442i	-0.1444+9.3969i	-0.2031+9.0587i
	30	$\overline{\beta_1}$	-0.3326+3.1744i	-0.3446+3.1742i	-1.1147+3.6824i	-1.2340+3.7502i
		$\overline{\beta_2}$	-0.4647+6.2550i	-0.5283+6.2350i	-1.9599+5.7909i	-2.0674+5.1729i
		$\overline{\beta_3}$	-0.0478+9.4219i	-0.0626+9.4197i	-0.1444+9.3969i	-0.1875+9.3721i
0.5	10	$\overline{\beta_1}$	-0.5108+3.1416i	-0.6617+3.0680i	-1.9459+3.1416i	-1.8301+2.2991i
		$\overline{\beta_2}$	0+6.2832i	0+6.2832i	0+6.2832i	0+6.2832i
		$\overline{\beta_3}$	-0.5108+9.4248i	-1.6761+8.1626i	-1.9459+9.4248i	-1.0926+6.6017i
	30	$\overline{\beta_1}$	-0.5108+3.1416i	-0.5279+3.1356i	-1.9459+3.1416i	-1.9958+2.9986i
		$\overline{\beta_2}$	0+6.2832i	0+6.2832i	0+6.2832i	0+6.2832i
		$\overline{\beta_3}$	-0.5108+9.4248i	-0.6780+9.3988i	-1.9459+9.4248i	-2.5840+8.4288i
0.7	10	$\overline{\beta_1}$	-0.3326+3.1744i	-0.4490+3.1663i	-1.1147+3.6824i	-1.8652+2.7424i
		$\overline{\beta_2}$	-0.4647+6.2550i	-0.9872+5.8387i	-1.9599+5.7909i	-0.6720+4.5281i
		$\overline{\beta_3}$	-0.0478+9.4219i	-0.2102+9.3442i	-0.1444+9.3969i	-0.2031+9.0587i
	30	$\overline{\beta_1}$	-0.3326+3.1744i	-0.3446+3.1742i	-1.1147+3.6824i	-1.2340+3.7502i
		$\overline{\beta_2}$	-0.4647+6.2550i	-0.5283+6.2350i	-1.9599+5.7909i	-2.0674+5.1729i
		$\overline{\beta_3}$	-0.0478+9.4219i	-0.0626+9.4197i	-0.1444+9.3969i	-0.1875+9.3721i

Fig. 11. Variation of damping ratio (ξ) with dimensionless damping coefficient D (η = 0.3, L = 10 nm)

Table 3 Characteristic values of nanorod for C-F boundary condition

			Dimensionless Damping Coefficient (D)			
			$\xi = 0.5$		$\xi = 1.5$	
η	L (nm)		$\mu=0$ nm^2	$\mu=2$ nm^2	$\mu=0$ nm^2	$\mu=2$ nm^2
0.3	10	$\overline{\beta_1}$	-0.1034+1.5793i	-0.1114+1.5796i	-0.3136+1.6625i	-0.3472+1.6707i
		$\overline{\beta_2}$	-0.5029+4.7284i	-0.8914+4.5744i	-2.1677+4.9632i	-1.9622+3.1264i
		$\overline{\beta_3}$	-0.2527+7.8278i	-0.6570+7.4139i	-0.7900+7.4916i	-0.3603+6.8108i
	30	$\overline{\beta_1}$	-0.1034+1.5793i	-0.1043+1.5793i	-0.3136+1.6625i	-0.3171+1.6634i
		$\overline{\beta_2}$	-0.5029+4.7284i	-0.5435+4.7215i	-2.1677+4.9632i	-2.4331+4.5761i
		$\overline{\beta_3}$	-0.2527+7.8278i	-0.3060+7.8105i	-0.7900+7.4916i	-0.8028+7.2631i
0.5	10	$\overline{\beta_1}$	-0.2554+1.5708i	-0.2746+1.5637i	-0.9730+1.5708i	-1.0051+1.4147i
		$\overline{\beta_2}$	-0.2554+4.7124i	-0.4559+4.6657i	-0.9730+4.7124i	-1.1215+3.7590i
		$\overline{\beta_3}$	-0.2554+7.8540i	-0.9220+7.5255i	-0.9730+7.8540i	-0.6012+6.3805i
	30	$\overline{\beta_1}$	-0.2554+1.5708i	-0.2575+1.5701i	-0.9730+1.5708i	-0.9810+1.5531i
		$\overline{\beta_2}$	-0.2554+4.7124i	-0.2754+4.7100i	-0.9730+4.7124i	-1.0979+4.6400i
		$\overline{\beta_3}$	-0.2554+7.8540i	-0.3128+7.8492i	-0.9730+7.8540i	-1.3783+7.5994i
0.7	10	$\overline{\beta_1}$	-0.4058+1.5368i	-0.4298+1.5150i	-1.5566+0.9318i	-1.3030+0.8760i
		$\overline{\beta_2}$	-0.0122+4.7120i	-0.0212+4.7112i	-0.0368+4.7089i	-0.0636+4.7006i
		$\overline{\beta_3}$	-0.2527+7.8801i	-1.3054+7.8292i	-0.7900+8.2164i	-1.4398+5.7877i
	30	$\overline{\beta_1}$	-0.4058+1.5368i	-0.4086+1.5345i	-1.5566+0.9318i	-1.5149+0.9222i
		$\overline{\beta_2}$	-0.0122+4.7120i	-0.0132+4.7119i	-0.0368+4.7089i	-0.0396+4.7083i
		$\overline{\beta_2}$	-0.2527+7.8801i	-0.3095+7.8888i	-0.7900+8.2164i	-0.9144+8.5625i
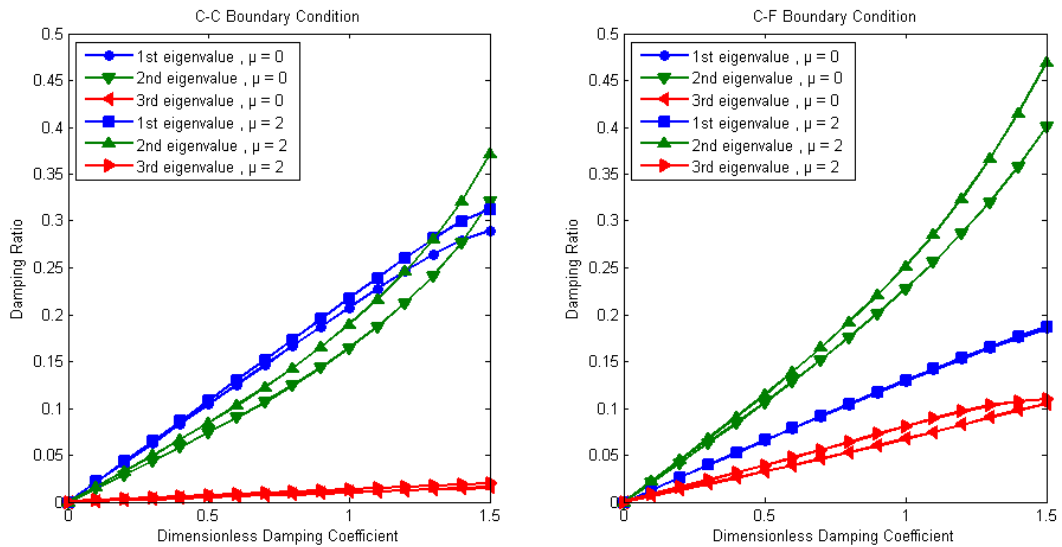
Fig. 12. Variation of damping ratio (ξ) with dimensionless damping coefficient D (η = 0.3, L = 30 nm)
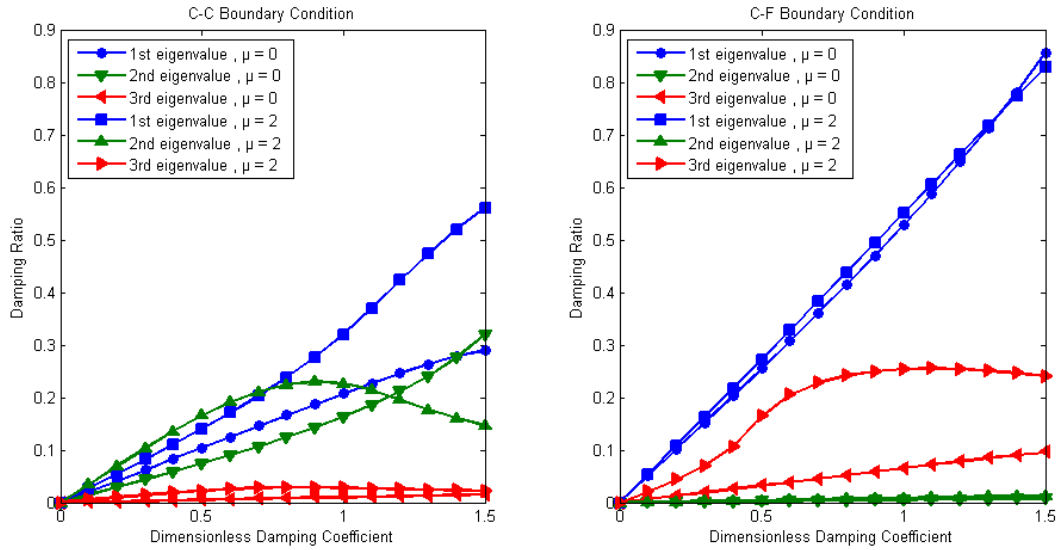
Fig. 13. Variation of damping ratio (ξ) with dimensionless damping coefficient D (η = 0.7, L = 10 nm)
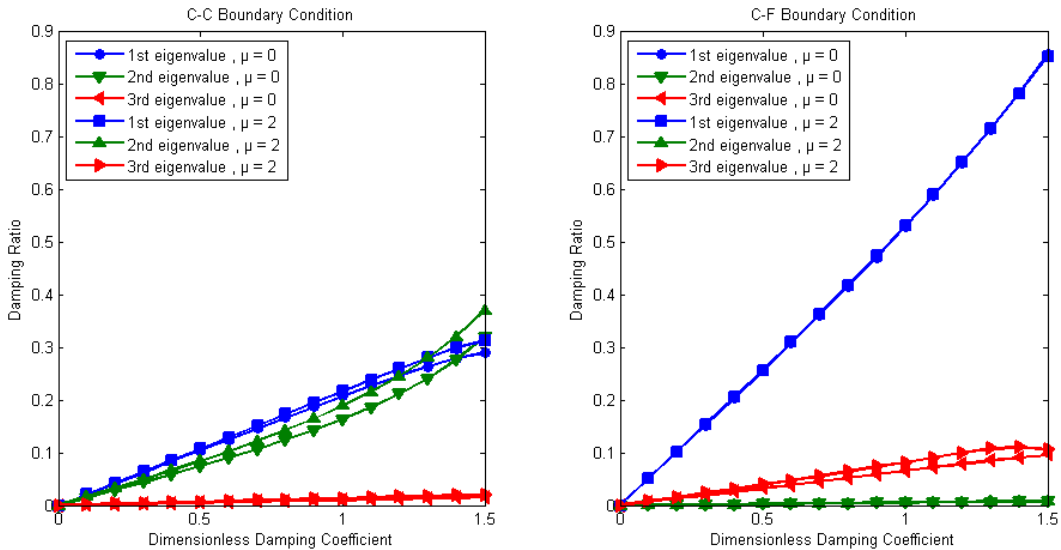
Fig. 14. Variation of damping ratio (ξ) with dimensionless damping coefficient D (η = 0.7, L = 30 nm)

Damping ratio (ξ) increases with increasing dimensionless damping coefficient (D) generally. Attachment point of damper increases damping ratio in C-F case when η is approaching to 1. In C-C case, damping ratio reaches maximum value at η = 0.5. For longer nanotube length, local and nonlocal damping ratios have very close values, since bigger nanotube length reduces the nonlocal effect.

4. Conclusions

Free longitudinal vibration of damped nanotube with attached a viscous damper is investigated in the present study. Effects of some parameters like dimensionless damping coefficient (D), nonlocal parameter (μ), attachment point of damper (η) and nanotube length (L) to the non-dimensional frequency (NDF), non-dimensional damping (NDD) and damping ratio (ξ) of nanorod is studied. Following results are obtained from the present study:

- The dimensionless damping coefficient (D) is effected by NDF differently depending on the attachment point of damper (η). NDD always increases with increasing D.
- The Nonlocal parameter (μ) has a decreasing effect on NDF whereas it has an increasing effect on NDD. Also μ is more effective in smaller nanotube length.
- NDD reaches a maximum value at $\eta = 0.5$ in C-C case and $\eta = 1$ in C-F case.
- Nanotube length (L) is effective only in nonlocal case ($\mu \neq 0$). NDF increases and NDD decreases with increasing L.
- Damping ratio (ξ) increases with increasing dimensionless damping coefficient (D) in C-F case. In C-C case, it reaches a maximum value at $\eta = 0.5$. Bigger nanotube length reduces nonlocal effect.

References

[1] Iijima, S., Helical microtubules of graphitic carbon, Nature, 354, 56–8, 1991. doi:10.1038/354056a0

[2] He, H., Pham-Huy, L.A., Dramou, P., Xiao, D., Zuo, P., Pham-Huy, C., Carbon nanotubes: Applications in pharmacy and medicine, BioMed Research International, 2013, 2013. doi:10.1155/2013/578290

[3] Marchesan, S., Kostarelos, K., Bianco, A., Prato, M., The winding road for carbon nanotubes in nanomedicine, Materials Today, 18, 12–9, 2015. doi:10.1016/j.mattod.2014.07.009

[4] Bourlon, B., Glattli, D.C., Miko, C., Forró, L., Bachtold, A., Carbon Nanotube Based Bearing for Rotational Motions, Nano Letters, 4, 709–12, 2004. doi:10.1021/nl035217g

[5] Kimoto, Y., Mori, H., Mikami, T., Akita, S., Nakayama, Y., Higashi, K., et al., Molecular Dynamics Study of Double-Walled Carbon Nanotubes for Nano-Mechanical Manipulation, Japanese Journal of Applied Physics, 44, 1641, 2005. doi:10.1143/JJAP.44.1641

[6] Von Oppen, F., Guinea, F., Mariani, E., Synthetic electric fields and phonon damping in carbon nanotubes and graphene, Physical Review B - Condensed Matter and Materials Physics, 80, 1–11, 2009. doi:10.1103/PhysRevB.80.075420

[7] Falk, K., Sedlmeier, F., Joly, L., Netz, R.R., Bocquet, L., Molecular origin of fast water transport in carbon nanotube membranes: Superlubricity versus curvature dependent friction, Nano Letters, 10, 4067–73, 2010. doi:10.1021/nl1021046

[8] Miyako, E., Kono, K., Yuba, E., Hosokawa, C., Nagai, H., Hagihara, Y., Carbon nanotube-liposome supramolecular nanotrains for intelligent molecular-transport systems., Nature Communications, 3, 1226, 2012. doi:10.1038/ncomms2233

[9] Eringen, A.C., Nonlocal polar elastic continua, International Journal of Engineering Science, 10, 1–16, 1972. doi:10.1016/0020-7225(72)90070-5

[10] Eringen, A.C., On differential equations of nonlocal elasticity and solutions of screw dislocation and surface waves, Journal of Applied Physics, 54, 4703–10, 1983. doi:10.1063/1.332803

[11] Khademolhosseini, F., Phani, A.S., Nojeh, A., Rajapakse, N., Nonlocal continuum modeling and molecular dynamics simulation of torsional vibration of carbon nanotubes, IEEE Transactions on Nanotechnology, 11, 34–43, 2012. doi:10.1109/TNANO.2011.2111380

[12] Aydogdu, M., Longitudinal wave propagation in multiwalled carbon nanotubes, Composite Structures, 107, 578–84, 2014. doi:10.1016/j.compstruct.2013.08.031

[13] Chen, C., Ma, M., Zhe Liu, J., Zheng, Q., Xu, Z., Viscous damping of nanobeam resonators: Humidity, thermal noise, and a paddling effect, Journal of Applied Physics, 110, 2011. doi:10.1063/1.3619854

[14] Wang, C.Y.Y., Li, C.F.F., Adhikari, S., Axisymmetric vibration of single-walled carbon nanotubes in water, Physics Letters A, 374, 2467–74, 2010. doi:10.1016/j.physleta.2010.04.002

[15] Rinaldi, S., Prabhakar, S., Vengallatore, S., Païdoussis, M.P., Dynamics of microscale pipes containing internal fluid flow: Damping, frequency shift, and stability, Journal of Sound and Vibration, 329, 1081–8, 2010. doi:10.1016/j.jsv.2009.10.025

[16] Ghavanloo, E., Daneshmand, F., Rafiei, M., Vibration and instability analysis of carbon nanotubes conveying fluid and resting on a linear viscoelastic Winkler foundation, Physica E: Low-Dimensional Systems and Nanostructures, 42, 2218–24, 2010. doi:10.1016/j.physe.2010.04.024

[17] Ghavanloo, E., Daneshmand, F., Amabili, M., Vibration analysis of a single microtubule surrounded by cytoplasm, Physica E: Low-Dimensional Systems and Nanostructures, 43, 192–8, 2010. doi:10.1016/j.physe.2010.07.016

[18] Ghavanloo, E., Rafiei, M., Daneshmand, F., In-plane vibration analysis of curved carbon nanotubes conveying fluid embedded in viscoelastic medium, Physics Letters A, 375, 1994–9, 2011. doi:10.1016/j.physleta.2011.03.025

[19] Ghavanloo, E., Fazelzadeh, S.A., Flow-thermoelastic vibration and instability analysis of viscoelastic carbon nanotubes embedded in viscous fluid, Physica E: Low-Dimensional Systems and Nanostructures, 44, 17–24, 2011. doi:10.1016/j.physe.2011.06.024

[20] Yun, K., Choi, J., Kim, S.-K., Song O, Flow-induced vibration and stability analysis of multi-wall carbon nanotubes, Journal of Mechanical Science and Technology, 26, 3911–20, 2012. doi:10.1007/s12206-012-0888-3

[21] Zeighampour, H., Tadi Beni, Y., Size-dependent vibration of fluid-conveying double-walled carbon nanotubes using couple stress shell theory, Physica E: Low-Dimensional Systems and Nanostructures, 61, 28–39, 2014. doi:10.1016/j.physe.2014.03.011

[22] Martin, M.J., Houston, B.H., Gas damping of carbon nanotube oscillators, Applied Physics Letters, 91, 103116, 2007. doi:10.1063/1.2779973

[23] Aydogdu, M., On the vibration of aligned carbon nanotube reinforced composite beams, Advances in Nano Research, 2, 199–210, 2014

[24] Chemi, A., Heireche, H., Zidour, M., Rakrak, K., Bousahla, A.A., Critical buckling load of chiral double-walled carbon nanotube using non-local theory elasticity, Advances in Nano

Research, 3, 193–206, 2015. doi:10.12989/anr.2015.3.4.193

[25] Aydogdu, M., Arda, M., Forced vibration of nanorods using nonlocal elasticity, Advances in Nano Research, 4, 265–79, 2016. doi:10.12989/anr.2016.4.4.265

[26] Soltani, P., Taherian, M.M., Farshidianfar, A., Vibration and instability of a viscous-fluid-conveying single-walled carbon nanotube embedded in a visco-elastic medium, Journal of Physics D: Applied Physics, 43, 425401, 2010. doi:10.1088/0022-3727/43/42/425401

[27] Zhen, Y.-X., Fang, B., Tang, Y., Thermal–mechanical vibration and instability analysis of fluid-conveying double walled carbon nanotubes embedded in visco-elastic medium, Physica E: Low-Dimensional Systems and Nanostructures, 44, 379–85, 2011. doi:10.1016/j.physe.2011.09.004

[28] Hoseinzadeh, M.S., Khadem, S.E., Thermoelastic vibration and damping analysis of double-walled carbon nanotubes based on shell theory, Physica E: Low-Dimensional Systems and Nanostructures, 43, 1146–54, 2011. doi:10.1016/j.physe.2011.01.013

[29] Hoseinzadeh, M.S., Khadem, S.E., A nonlocal shell theory model for evaluation of thermoelastic damping in the vibration of a double-walled carbon nanotube, Physica E: Low-Dimensional Systems and Nanostructures, 57, 6–11, 2014. doi:10.1016/j.physe.2013.10.009

[30] Hajnayeb, A., Khadem, S.E., Zamanian, M., Thermoelastic damping of a double-walled carbon nanotube under electrostatic force, Micro & Nano Letters, 6, 698, 2011. doi:10.1049/mnl.2011.0193

[31] Schmid, D.R., Stiller, P.L., Strunk, C., Hüttel, a K., Magnetic damping of a carbon nanotube nano-electromechanical resonator, New Journal of Physics, 14, 83024, 2012. doi:10.1088/1367-2630/14/8/083024

[32] Chang, W.-J., Lee, H.-L., Vibration analysis of viscoelastic carbon nanotubes, Micro & Nano Letters, 7, 1308–12, 2012. doi:10.1049/mnl.2012.0612

[33] Hizal, N.A., Gürgöze, M., Lumped parameter representation of a longitudinally vibrating elastic rod viscously damped in-span, Journal of Sound and Vibration, 216, 328–36, 1998. doi:10.1006/jsvi.1998.1685

[34] Yüksel, Ş., Gürgöze, M., Continuous and discrete models for longitudinally vibrating elastic rods viscously damped in-span, Journal of Sound and Vibration, 257, 996–1006, 2002. doi:10.1006/jsvi.5032

[35] Yüksel, Ş., Dalli, U., Longitudinally vibrating elastic rods with locally and non-locally reacting viscous dampers, Shock and Vibration, 12, 109–18, 2005

[36] Zhou, Z., Qian, D., Yu, M.-F., A Computational Study on the Transversal Visco-Elastic Properties of Single Walled Carbon Nanotubes and Their Relation to the Damping Mechanism, Journal of Computational and Theoretical Nanoscience, 8, 820–30, 2010

[37] Jeong, B., Cho, H., Yu, M.-F., Vakakis, A.F., McFarland, D.M., Bergman, L.A., Modeling and Measurement of Geometrically Nonlinear Damping in a Microcantilever–Nanotube System, ACS Nano, 7, 8547–53, 2013. doi:10.1021/nn402479d

[38] Adhikari, S., Murmu, T., McCarthy, M.A., Dynamic finite element analysis of axially vibrating nonlocal rods, Finite Elements in Analysis and Design, 63, 42–50, 2013. doi:10.1016/j.finel.2012.08.001

[39] Lei, Y., Adhikari, S., Murmu, T., Friswell, M.I., Asymptotic frequencies of various damped nonlocal beams and plates, Mechanics Research Communications, 62, 94–101, 2014. doi:10.1016/j.mechrescom.2014.08.002

[40] Ghorbanpour Arani, A., Amir, S., Dashti, P., Yousefi, M., Flow-induced vibration of double bonded visco-CNTs under magnetic fields considering surface effect, Computational Materials Science, 86, 144–54, 2014. doi:10.1016/j.commatsci.2014.01.047

[41] Karličić, D., Cajić, M., Murmu, T., Adhikari, S., Nonlocal longitudinal vibration of viscoelastic coupled double-nanorod systems, European Journal of Mechanics - A/Solids, 49, 183–96, 2015. doi:10.1016/j.euromechsol.2014.07.005

[42] Erol, H., Gürgöze, M., Longitudinal vibrations of a double-rod system coupled by springs and dampers, Journal of Sound and Vibration, 276, 419–30, 2004. doi:10.1016/j.jsv.2003.10.043

[43] Buchoux, J., Aimé, J.-P., Boisgard, R., Nguyen, C.V., Buchaillot, L., Marsaudon, S., Investigation of the carbon nanotube AFM tip contacts: free sliding versus pinned contact., Nanotechnology, 20, 475701/8pp, 2009. doi:10.1088/0957-4484/20/47/475701

[44] Eichler, A., Moser, J., Chaste, J., Zdrojek, M., Wilson-Rae, I., Bachtold, A., Nonlinear damping in mechanical resonators made from carbon nanotubes and graphene, Nat Nano, 6, 339–42, 2011

[45] Li, J., Bi, K., Chen, M., Chen, Y., The oscillatory damped behavior of double wall carbon nanotube oscillators in gaseous environment, Science in China, Series E: Technological Sciences, 52, 916–21, 2009. doi:10.1007/s11431-009-0073-9

[46] Barnard, A.W., Sazonova, V., van der Zande, A.M., McEuen, P.L., Fluctuation broadening in carbon nanotube resonators., Proceedings of the National Academy of Sciences of the United States of America, 109, 19093–6, 2012. doi:10.1073/pnas.1216407109

[47] Hüttel, A.K., Steele, G.A., Witkamp, B., Poot, M., Kouwenhoven, L.P., Van Der Zant, H.S.J., Carbon nanotubes as ultrahigh quality factor mechanical resonators, Nano Letters, 9, 2547–52, 2009. doi:10.1021/nl900612h

[48] Aydogdu, M., Elishakoff, I., On the vibration of nanorods restrained by a linear spring in-span, Mechanics Research Communications, 57, 90–6, 2014. doi:10.1016/j.mechrescom.2014.03.003